*P*roduction *E*ngineering & *D*esign For *D*evelopment, ***PEDD7***,
Cairo, February 7 – 9, 2006

FINITE ELEMENT ANALYSIS OF SLOSHING IN LIQUID-FILLED CONTAINERS

Mustafa Arafa
Lecturer, Department of Mechanical Design and Production Engineering, Cairo University, Cairo, Egypt
mharafa@gmail.com, mharafa@yahoo.com

ABSTRACT

The focus of the present paper is on the development of a finite element formulation to investigate the sloshing of liquids in partially filled rigid rectangular tanks undergoing base excitation. The liquid domain is discretized into two-dimensional four-node rectangular elements with the liquid velocity potential representing the nodal degrees of freedom. Liquid sloshing effects induced by both steady-state harmonic and arbitrary horizontal base excitation are investigated in terms of the slosh frequencies, liquid velocity field, free surface displacement and hydrodynamic forces acting on the tank walls. The model is employed to study the effects of inserting a bottom-mounted vertical rigid baffle, as well as side-mounted horizontal baffles that are wholly immersed in the liquid region, in an attempt to investigate their viability in acting as slosh suppression devices.

KEYWORDS
Sloshing, finite element analysis, partially filled tanks, fluid—structure interaction.

1. INTRODUCTION

Sloshing is known as the oscillation of the free surface of a liquid in an externally excited container. Partially filled liquid tanks undergoing accelerated motions are susceptible to slosh-induced loads, which may affect the dynamic behavior of the liquid-retaining structure, and may even be severe enough to cause structural damage. Sloshing of liquids in moving containers is of practical concern in many engineering applications, such as fuel sloshing in aircraft tanks as a result of sharp flight maneuvers, liquid sloshing in large storage tanks due to earthquakes and fluid oscillation in tanker trucks traveling on highways.

An extensive research has been conducted in the past four decades to investigate the motion of liquids in rigid and deformable containers. Early simulations of the liquid sloshing problem relied upon constructing mechanical analogies that comprise pendulums or spring—mass elements whose parameters are designed to simulate the resultant dynamic pressure loads imparted on a tank during sloshing for various tank geometries and fluid characteristics [1]. For a comprehensive review of the phenomenon of sloshing, including analytical predictions and experimental observations, the reader is referred to the work of Abramson [2]. More recent studies aim at developing numerical models to investigate the fluid—structure interaction of the liquid-coupled system [3-7]. Several means are adopted in practice to overcome the undesirable effects of sloshing [8, 9]. A common technique is to provide the

tank with baffles or separators in order to reduce the bulk motion of the contained liquid during sloshing and also to introduce some energy dissipation due to flow separation effects as the liquid oscillates past these baffles or other obstacles in the tank [10-15].

This paper presents a finite element formulation to study the sloshing of liquids in externally excited rigid rectangular tanks. The analysis aims at studying the dynamic behavior of partially filled liquid-retaining structures with and without rigid baffles that are placed within the liquid region. The formulation relies upon discretizing the liquid domain into two-dimensional four-node elements, with the liquid velocity potential being the nodal degrees of freedom. Fluid—structure interaction is included in the model to couple the liquid motion with the rigid tank walls to ensure continuity of liquid and structural motion at the liquid—tank interface. Liquid sloshing effects induced by both steady-state harmonic and arbitrary horizontal base excitation are investigated in terms of the slosh frequencies, liquid velocity field, free surface displacement and hydrodynamic forces acting on the tank walls. Effects of introducing a bottom-mounted vertical baffle, as well as side-mounted horizontal baffles that are wholly immersed in the liquid domain are investigated.

The remainder of this paper is divided into four sections. First, a statement of the problem, together with the basic governing equations, is given. Next, the finite element model that is developed to study sloshing of liquids in rectangular rigid containers is presented. The final two sections present numerical examples, conclusions and areas where future research could be directed.

2. PROBLEM STATEMENT AND GOVERNING EQUATIONS

Figure 1 shows a schematic diagram of the liquid—tank system under consideration. A rigid rectangular tank of length L is partially filled with liquid to a height H. Owing to the two-dimensional geometry of the problem, a Cartesian coordinate system is employed to describe the position of any point belonging to the liquid domain. The free surface displacement, measured from the undisturbed liquid surface at equilibrium, is denoted by $\eta(x,t)$. Effects of the liquid compressibility, viscosity and surface tension are neglected in the present study. The tank is also equipped with a vertical bottom-mounted baffle of height h, placed at a distance l from the left tank wall, as indicated. The baffle is assumed to be thin, rigid and wholly immersed in the liquid region.

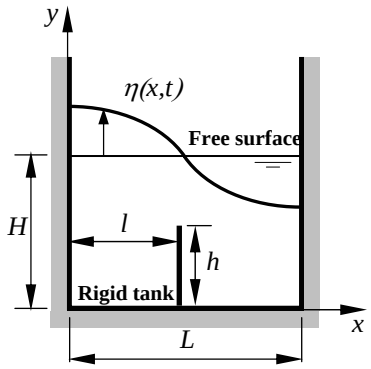

Fig. 1. Rigid rectangular tank and coordinate system.

The equation governing the irrotational motion of an inviscid incompressible fluid is given in terms of the velocity potential $\phi(x,y,t)$ as:

$$\nabla^2\phi = 0 \tag{1}$$

The liquid velocity $\vec{v}(x,y,t)$ relates to the velocity potential through:

$$\vec{v} = \nabla\phi \tag{2}$$

For the case of free vibrations of the liquid in a fixed rigid container without baffles, the solution of Eq. (1) in the region occupied by the liquid must satisfy the proper boundary conditions. Prescribed normal velocities are imposed on the fluid particles adjacent to the rigid tank surfaces. Thus at the rigid tank bottom, y=0, the liquid velocity in the vertical direction vanishes:

$$\frac{\partial\phi}{\partial y}(x,0,t) = 0 \tag{3}$$

At the rigid tank walls, $x = 0$ and $x = L$, the liquid velocity in the horizontal direction vanishes:

$$\frac{\partial\phi}{\partial x}(0,y,t) = 0 \quad , \quad \frac{\partial\phi}{\partial x}(L,y,t) = 0 \tag{4, 5}$$

At the liquid free surface, assuming small-amplitude motion, the boundary conditions are defined after Haroun and Housner [16] as:

$$\frac{\partial\phi}{\partial y}(x,H,t) = \frac{\partial\eta}{\partial t}(x,t) \quad , \quad \rho\frac{\partial\phi}{\partial t}(x,H,t) + \rho g\eta(x,t) = 0 \tag{6,7}$$

This formulation can be employed to investigate the behavior of the coupled liquid—rigid tank—surface-wave system, and forms the basis of the finite element model described in the following section.

3. FINITE ELEMENT FORMULATION

The finite element model developed in this work relies upon discretizing the liquid domain into four-noded rectangular elements, with the liquid velocity potential being the only degree of freedom at each node. The velocity potential at any point within the liquid element is interpolated by:

$$\phi(x,y) = \alpha_1 + \alpha_2 x + \alpha_3 y + \alpha_4 xy \tag{8}$$

Accordingly, the velocity potential at any point in the fluid element can be expressed in terms of the nodal degrees of freedom as:

$$\phi(x,y) = \{N(x,y)\}\{\phi^e\} \tag{9}$$

where $\{N(x,y)\}$ is the vector of shape functions and $\{\phi^e\}$ is the nodal degrees of freedom vector. As the liquid under consideration is incompressible, the potential energy of a liquid element consists only of a gravitational potential energy term:

$$U^e = \frac{1}{2}\rho bg\int_0^a \eta^2(x,t)dx \tag{10}$$

where ρ is the liquid density, b is the out-of-plane width of the tank, g is the gravitational acceleration, a is the element length, and the integration is carried out over all elements belonging to the free surface. The kinetic energy of a liquid element is expressed as:

$$T^e = \frac{1}{2}\rho\int_V (\nabla\phi)^2 dV \tag{11}$$

where V is the element volume. Imposing the shape functions as defined in Eq. (9) and substituting into Eq. (11) yields:

$$T^e = \frac{1}{2}\rho b\left\{\phi^e\right\}^T \int_0^d\int_0^a \left[\left\{N_x\right\}^T\left\{N_x\right\} + \left\{N_y\right\}^T\left\{N_y\right\}\right]dxdy\left\{\phi^e\right\} \tag{12}$$

where the subscripts x and y denote partial differentiation with the respective variable, and d is the element height. Accordingly, the stiffness matrix of the liquid element is given by:

$$\left[K^e\right] = \rho b\int_0^d\int_0^a \left[\left\{N_x\right\}^T\left\{N_x\right\} + \left\{N_y\right\}^T\left\{N_y\right\}\right]dxdy \tag{13}$$

From Eqs. (7) and (9), the free surface displacement can be expressed in terms of the liquid velocity potential as:

$$\eta(x) = -\frac{1}{g}\left\{N(x,d)\right\}\left\{\dot{\phi}\right\} \tag{14}$$

where the time dependence is dropped for brevity. Hence the liquid element potential energy is expressed as:

$$U^e = \frac{1}{2}\frac{\rho b}{g}\left\{\dot{\phi}\right\}^T \int_0^a \left\{N(x,d)\right\}^T\left\{N(x,d)\right\}\left\{\dot{\phi}\right\}dx \tag{15}$$

from which the liquid element mass matrix is given by:

$$\left[M^e\right] = \frac{\rho b}{g}\int_0^a \left\{N(x,d)\right\}^T\left\{N(x,d)\right\}dx \tag{16}$$

In order to include the rigid enclosure in the present finite element formulation, three spring-supported pistons are attached to the liquid domain, as depicted in Fig. 2. Mass and stiffness parameters of the additional mass—spring systems are selected to ensure the walls of the container are practically rigid and possess natural frequencies that are appreciably higher than the frequency range of interest which includes the liquid slosh frequencies. Normal displacements of all liquid particles lying on the tank boundaries are coupled to the displacements w_I, w_{II}, w_{III} of the pistons. In order to impose this condition, the work done by the liquid pressure forces on the spring-supported pistons can be expressed by:

$$W_d = -\rho\int_{A_I} \dot{\phi}_I w_I\, dA_I - \rho\int_{A_{II}} \dot{\phi}_{II} w_{II}\, dA_{II} - \rho\int_{A_{III}} \dot{\phi}_{III} w_{III}\, dA_{III} \tag{17}$$

where the integrals are carried out along all the fluid—structure interface areas, commonly known as the 'wetted areas', designated A_I, A_{II}, A_{III}.

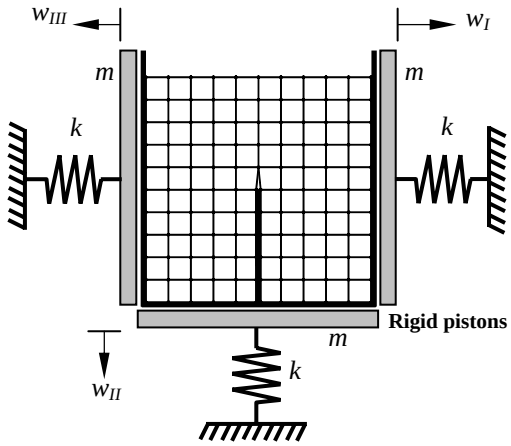

Fig. 2. Modeling of the tank walls as rigid spring-supported pistons.

Inserting the shape functions as defined in Eq. (9) and substituting into Eq. (17) yields:

$$W_d^e = -w_I \left\{\Omega_I^e\right\}\left\{\ddot{\phi}\right\} - w_{II} \left\{\Omega_{II}^e\right\}\left\{\ddot{\phi}\right\} - w_{III} \left\{\Omega_{III}^e\right\}\left\{\ddot{\phi}\right\} \tag{18}$$

where

$$\left\{\Omega_I^e\right\} = \rho\int_0^d \left\{N(a,y)\right\} b dy\,, \quad \left\{\Omega_{II}^e\right\} = \rho\int_0^a \left\{N(x,0)\right\} b dx\,, \quad \left\{\Omega_{III}^e\right\} = \rho\int_0^d \left\{N(0,y)\right\} b dy$$

are the fluid—structure coupling vectors. The element equations of motion are then obtained by using Lagrange's equation. Upon assembly, the equations of motion for the entire liquid-coupled system are expressed as:

$$\begin{bmatrix} [M] & -\rho\{\Omega_I\}^T & -\rho\{\Omega_{II}\}^T & -\rho\{\Omega_{III}\}^T \\ 0 & \rho m & 0 & 0 \\ 0 & 0 & \rho m & 0 \\ 0 & 0 & 0 & \rho m \end{bmatrix} \begin{Bmatrix} \{\ddot{p}\} \\ \ddot{w}_I \\ \ddot{w}_{II} \\ \ddot{w}_{III} \end{Bmatrix} + \begin{bmatrix} [K] & 0 & 0 & 0 \\ -\{\Omega_I\} & \rho k & 0 & 0 \\ -\{\Omega_{II}\} & 0 & \rho k & 0 \\ -\{\Omega_{III}\} & 0 & 0 & \rho k \end{bmatrix} \begin{Bmatrix} \{p\} \\ w_I \\ w_{II} \\ w_{III} \end{Bmatrix} = \begin{Bmatrix} \{0\} \\ 0 \\ 0 \\ 0 \end{Bmatrix} \tag{19}$$

where $\{p\}$ is the vector of liquid nodal pressures. Elements of the liquid mass matrix $[M]$ have contributions only from the nodes belonging to the free surface. Hence it becomes appropriate to separate the degrees of freedom corresponding to nodes lying on the free surface from the total degrees of freedom. In this way, the equations of motion of the liquid domain are expressed as:

$$\begin{bmatrix} [M_{ff}] & 0 \\ 0 & 0 \end{bmatrix} \begin{Bmatrix} \{\ddot{p}_f\} \\ \{\ddot{p}_r\} \end{Bmatrix} + \begin{bmatrix} [K_{ff}] & [K_{fr}] \\ [K_{rf}] & [K_{rr}] \end{bmatrix} \begin{Bmatrix} \{p_f\} \\ \{p_r\} \end{Bmatrix} = \rho \begin{Bmatrix} \{\Omega_{If}\}^T \ddot{w}_I + \{\Omega_{IIIf}\}^T \ddot{w}_{III} \\ \{\Omega_{Ir}\}^T \ddot{w}_I + \{\Omega_{IIr}\}^T \ddot{w}_{II} + \{\Omega_{IIIr}\}^T \ddot{w}_{III} \end{Bmatrix} \tag{20}$$

where the mass and stiffness matrices are accordingly partitioned, and subscripts *f* and *r* are introduced to identify entities pertaining to the free surface and those belonging elsewhere in the liquid region, respectively. The vector of liquid pressures at nodes not belonging to the free surface, $\{p_r\}$, can then be eliminated from the second set of equations in (20). After some algebraic manipulation, the resulting equations of motion can be expressed in the form:

$$\begin{bmatrix} [M_{ff}] & \{M_{12}\} & \{M_{13}\} & \{M_{14}\} \\ 0 & m_{22} & m_{23} & m_{24} \\ 0 & m_{32} & m_{33} & m_{34} \\ 0 & m_{42} & m_{43} & m_{44} \end{bmatrix} \begin{Bmatrix} \{\ddot{p}_f\} \\ \ddot{w}_I \\ \ddot{w}_{II} \\ \ddot{w}_{III} \end{Bmatrix} + \begin{bmatrix} [K_{11}] & 0 & 0 & 0 \\ \{K_{21}\} & \rho k & 0 & 0 \\ \{K_{31}\} & 0 & \rho k & 0 \\ \{K_{41}\} & 0 & 0 & \rho k \end{bmatrix} \begin{Bmatrix} \{p_f\} \\ w_I \\ w_{II} \\ w_{III} \end{Bmatrix} = \begin{Bmatrix} \{0\} \\ \rho f_I \\ \rho f_{II} \\ \rho f_{III} \end{Bmatrix} \tag{21}$$

Solution of the eigenvalue problem thus entails handling reduced-size matrices, as only the degrees of freedom of the free surface nodes need to be considered, along with three additional displacements describing the motion of the rigid tank walls. Modeling of the baffle is accounted for by introducing a fourth mass—spring element, together with an additional displacement, $w_{IV}(t)$. The model is then used to determine the liquid slosh frequencies in fixed tanks, as well as the forced response of the system under tank wall movement.

4. NUMERICAL RESULTS AND DISCUSSION

The finite element formulation described in the previous section is employed to study the free and forced sloshing characteristics of water (ρ =1000 kg/m^3) in a rigid rectangular tank. The width *b* is taken as unity in all cases. The liquid region is divided into 20 by 20 elements. The liquid natural frequencies and mode shapes are obtained for a fixed tank, both with and without a rigid baffle, placed at various locations, and extending vertically to different

heights. Harmonic base excitation is then applied horizontally to the tank rigid walls, and the resultant hydrodynamic forces exerted on the tank walls are obtained. The model is then extended to handle side-mounted horizontal baffles and arbitrary base excitation schemes.

Example 1: Slosh frequencies in a fixed tank.

As a first illustrative example to verify the accuracy of the present formulation, the liquid slosh frequencies are calculated for a rectangular tank with L=2m, H=1m. Table 1 lists the first five natural frequencies, in comparison with the analytical solution presented by Abramson [2]. The results are shown to be in good agreement, with a percentage error below 2% up to the fifth mode. Higher frequencies can be predicted more accurately by increasing the number of elements. Figure 3 shows the liquid velocity field in the unbaffled tank at the first two slosh modes, as obtained from the present finite element analysis. The liquid velocity vectors shown are the average element velocities evaluated at the center of each element used in the mesh. Liquid particles adjacent to boundaries of the tank are shown to possess velocity vectors that are parallel to the boundary surfaces.

Table 1. Liquid slosh frequencies in a fixed tank (L=2m, H=1m)

Mode	*Natural frequencies [rad/s]*	
	Present	Abramson [2]
1	3.7626	3.7594
2	5.5558	5.5411
3	6.8382	6.7986
4	7.9323	7.8510
5	8.9204	8.7777

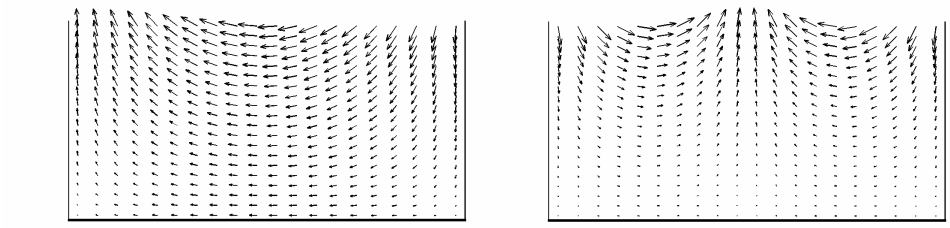

(a) (b)

Fig. 3. Liquid velocity field at the (a) first and (b) second slosh mode.

Example 2: Horizontally excited tank.

The tank of the previous example is now subjected to a prescribed steady-state harmonic horizontal base excitation of the form $w_I(t) = We^{i\omega t}$, $w_{III}(t) = \pm We^{i\omega t}$. The left tank wall can be made to move either in-phase or out-of-phase with the opposing wall, as set by the relative sign of $w_{III}(t)$. Motion of the tank bottom is set equal to zero. Time response is obtained by numerical integration of the equations of motion using the Newmark scheme. Figure 4 shows the non-dimensional time history plot of the free surface displacement, evaluated for liquid particles lying at the left wall of the tank, under the two base excitation frequencies

$\omega/\omega_1 = 1.1$ and $\omega/\omega_1 = 0.999$, ω_1 being the fundamental slosh frequency. The non-dimensional time is expressed as $t\sqrt{\frac{g}{H}}$ while the free surface displacement is expressed in a dimensionless form by $\frac{\eta(0,t)}{W}$. The amplitude of base motion is taken as 1.86 mm. Results of the present analysis are almost in exact agreement with those presented by Wu *et al.* [4]. The plots also match similar predictions reported by Frandsen and Borthwick [7].

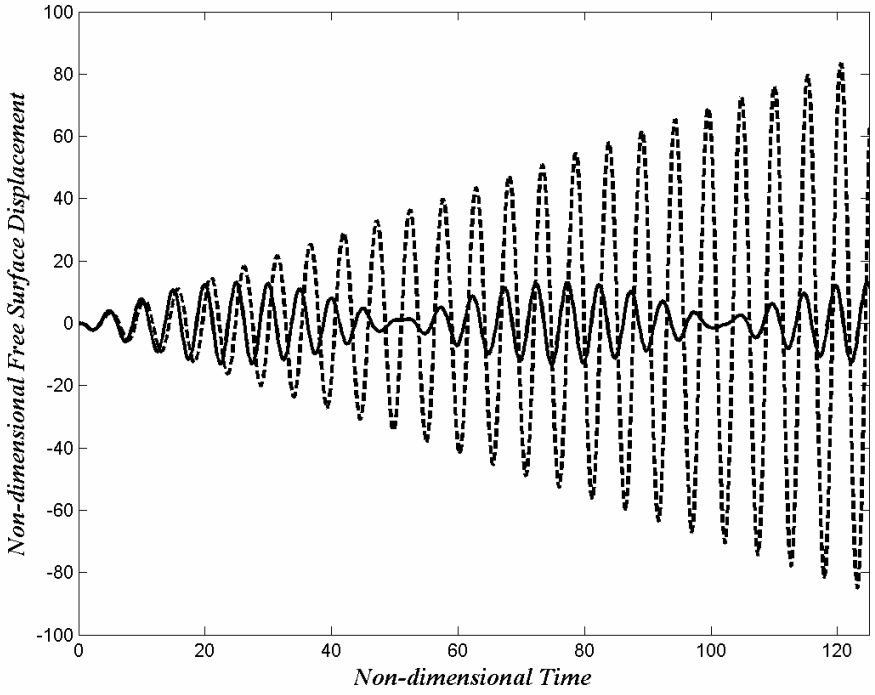

Fig. 4. Time response of free surface displacement at left wall (L=2 m, H=1 m, W=1.86 mm).
—— , $\omega/\omega_1 = 1.1$; – – , $\omega/\omega_1 = 0.999$.

Example 3: Sloshing in a baffled tank.

The above formulation is extended to include the effects of providing the tank with a rigid bottom-mounted vertical baffle that is wholly submerged in the liquid. In this case, the fluid—structure interaction between the baffle and neighboring liquid entities is handled by defining a fourth coupling vector $\left\{\Omega_{IV}^{e}\right\}$ to enforce coupling of the liquid and baffle displacements at the liquid—baffle interface. In a sense, the baffle acts to split part of the liquid domain into neighboring regions, and consequently, it becomes necessary to introduce additional liquid nodes into the finite element model in order to have liquid nodes lying on both sides of the baffle, as indicated in Fig. 2. The number of elements, though, for both the unbaffled and baffled tanks is the same. The tank considered in this example has the dimensions L=30m and H=15m, to enable comparison with the results reported by Choun and Yun [13].

Figure 5 shows the variation of the first three slosh frequencies versus baffle height, expressed in a non-dimensional form through division by the liquid depth. The results, which correspond to a baffle that is placed midway along the tank length, are compared with

predictions by Choun and Yun [13] and Evans and McIver [15], who investigated the effects of a vertical baffle on the eigenfrequencies of fluid in a rectangular container using the linearized theory of water waves. The general trend is a decrease in slosh frequencies with increasing baffle height for the first and third modes. The same pattern was obtained in the above two references, with results of the present analysis matching more closely those of Evans and McIver [15] for the fundamental slosh frequency.

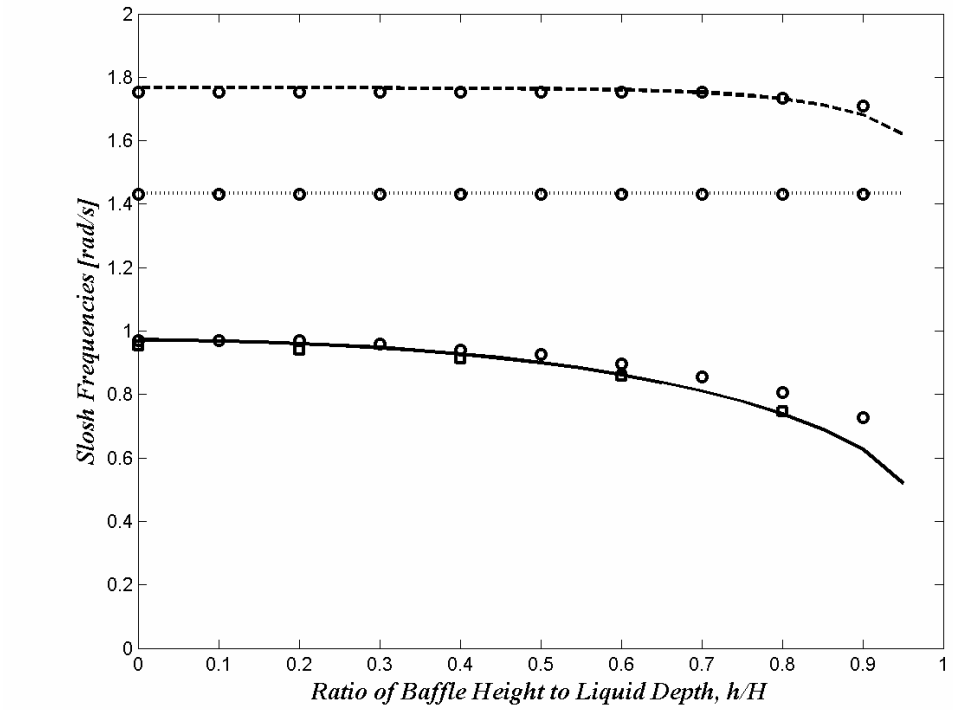

Fig. 5. Variation of slosh frequencies with baffle height (L=30 m, H=15 m, l/L=0.5). ——— ω_1; – – – ω_2; ····· , ω_3; O, Choun and Yun [13]; □ Evans and McIver [15].

Figure 6 shows the liquid velocity field at the first two slosh modes throughout a tank which is provided with a baffle, placed midway along the tank length and submerged by one-half the liquid height. Liquid motion at the tip of the baffle features a slight swirl at the first mode.

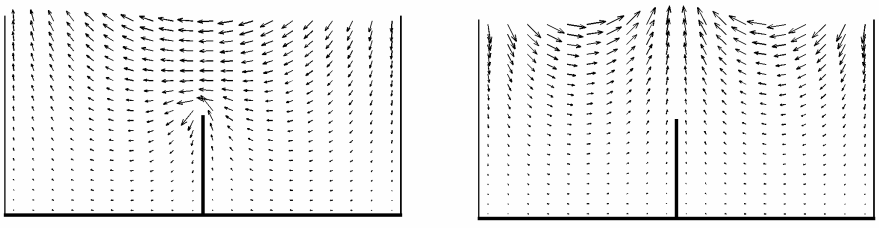

(a) (b)

Fig. 6. Velocity field in a baffled tank at the (a) first, and (b) second slosh mode (l/L=0.5, h/H=0.5).

Example 4: Tank with horizontal baffles.

A tank with horizontal baffles is now investigated. The configuration is shown in Fig. 7. Two identical rigid baffles are fitted to the opposite side walls of the tank. The analysis follows directly from the formulation presented above.

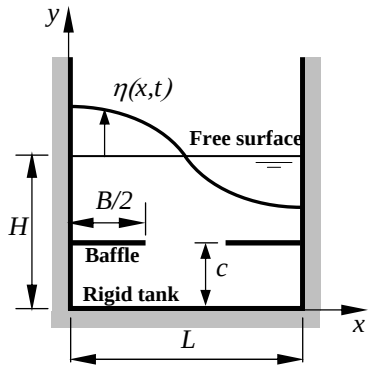

Fig. 7. Rectangular tank with horizontal baffles.

Figure 8 shows the liquid velocity field at the first two slosh modes throughout the tank. The horizontal baffles are placed at a height of 70% of the total liquid depth, measured from the tank bottom, and the combined length of the two baffles covers 60% of the tank length. Liquid motion beneath the horizontal baffles is significantly reduced.

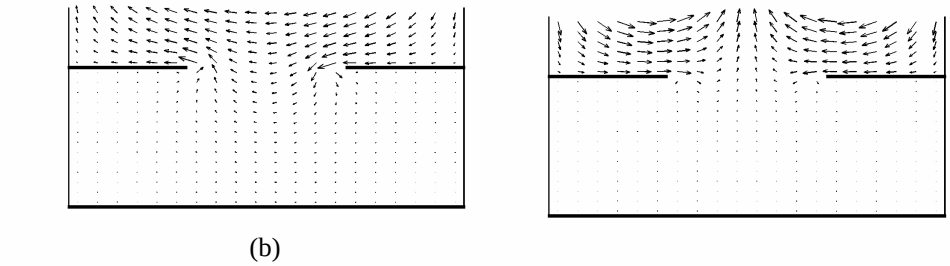

(b)

Fig. 8. Liquid velocity field in a tank with horizontal baffles at the (a) first, and (b) second slosh mode (B/L=0.6, c/H=0.7).

Figure 9 shows the variation of the fundamental slosh frequency with baffle location for various baffle sizes. Baffles extending over longer spans and placed closer to the liquid free surface have a greater influence on lowering the fundamental slosh frequency. The limiting case is when the two baffles are placed at the free surface and extended horizontally to meet one another, entirely trapping the liquid, in which case the liquid behaves like a rigid body as if it were frozen.

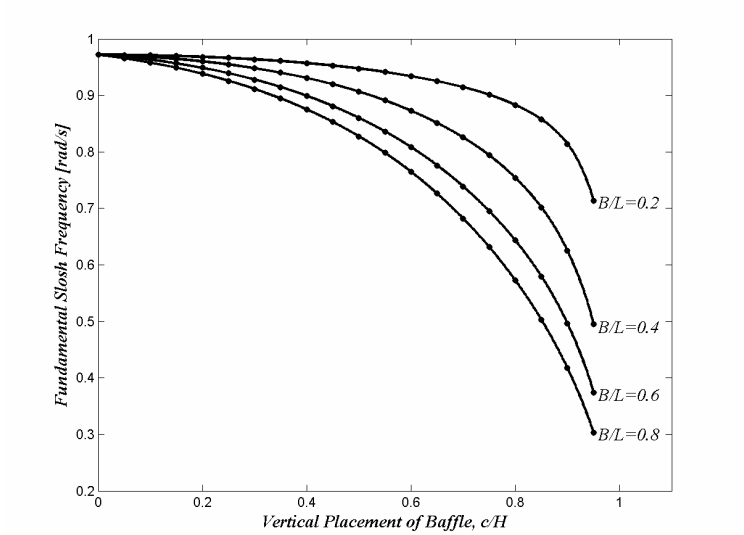

Fig. 9. Fundamental slosh frequency versus baffle location for various baffle sizes. (*L*=30 m, *H*=15 m*).*

Example 5: Arbitrary excitation.

In this example, the tank is subjected to an arbitrary input excitation, and a comparison of the tank behavior for various baffle configurations is made. The chosen input base motion is a 'relaxed' step input, in which the tank displacement during rise time is given by:

$$w_I(t) = -w_{III}(t) = \frac{W_s}{2}\left(1 - \cos\frac{\pi t}{t_r}\right) \tag{22}$$

where W_s and t_r denote the steady-state displacement and rise time, respectively. Figure 10 shows the time response of the resultant hydrodynamic forces acting on the tank walls for the cases of an unbaffled tank, a tank provided with a vertical baffle, and one with horizontal baffles, all evaluated for W_s=1m and t_r=5s. For the particular configurations chosen, it is shown that significant reduction (almost 50%) in the induced hydrodynamic forces can be attained by introducing horizontal baffles in the tank design. A 30% reduction in forces is achieved with a single vertical baffle.

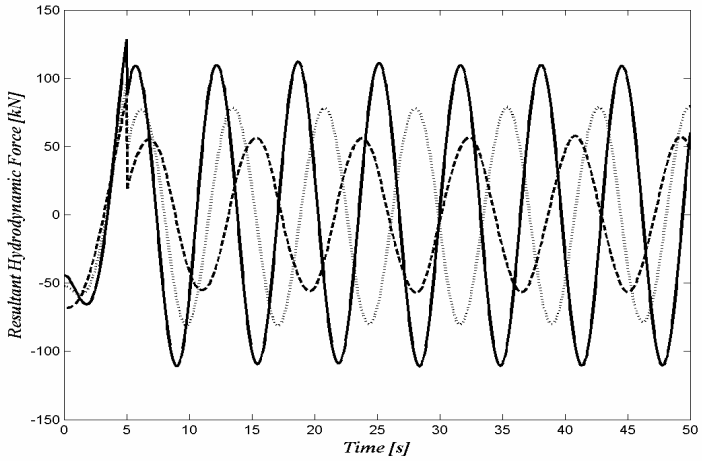

Fig. 10. Resultant hydrodynamic force acting on tank walls (*L*=30 m, *H*=15m, W_s=1m, t_r=5s). ——— , unbaffled tank; ····· , tank with a vertical baffle (*l/L*=0.5, *h/H*=0.6); – – , tank with horizontal baffles (*B/L*=0.6, *c/H*=0.7).

5. CONCLUSIONS

This paper presented a finite element formulation of the fluid—structure interaction problem to study the sloshing behavior of liquids in rigid rectangular tanks. Liquid sloshing effects induced by horizontal base excitation are investigated in terms of the slosh frequencies, liquid velocity field, free surface displacement and hydrodynamic forces acting on the tank walls. Results of the present work compare quite favorably with established predictions reported in the literature. The model is employed to study the effects of inserting both vertical and horizontal rigid baffles within the liquid domain on the slosh frequencies and free surface motion during forced vibration, in an attempt to investigate their viability in acting as slosh suppression devices. Numerical simulations indicate that significant reduction in the hydrodynamic forces is achieved for baffled tanks subjected to various external excitation schemes.

REFERENCES

1. **Housner, G.W.,** "Dynamic Pressures on Accelerated Fluid Containers," Bulletin of the Seismological Society of America, Vol. 47, pp. 15-35, 1957.
2. **Abramson, H.N.,** The Dynamic Behavior of Liquids in Moving Containers, NASA SP-106, Washington, D.C., 1966, updated by Dodge, F.T., Southwest Research Institute, 2000.
3. **Frandsen, J.B.,** "Sloshing Motions in Excited Tanks," Journal of Computational Physics, Vol. 196, Issue 1, 53-87, 2004.
4. **Wu, G.X., Ma, Q.W. and Taylor, R.E.,** "Numerical Simulation of Sloshing Waves in a 3D Tank based on a Finite Element Method," Applied Ocean Research, 20, 337-355, 1998.
5. **Pal, N.C., Bhattacharyya, S.K. and Sinha, P.K.,** " Non-linear Coupled Slosh Dynamics of Liquid-filled Laminated Composite Containers: A Two Dimensional Finite Element Approach," Journal of Sound and Vibration, 261(4), 729-749, 2003.
6. **Çelebi, M.S. and Akyildiz, H.,** "Nonlinear Modelling of Liquid Sloshing in a Moving Rectangular Tank," Ocean Engineering, Vol. 29, Issue 12, 1527-1553, 2002.
7. **Frandsen, J.B. and Borthwick, A.G.L.,** "Free and Forced Sloshing Motions in a 2-D Numerical Wave Tank," Proceedings of OMAE'02: The 21st International Conference on Offshore Mechanics and Arctic Engineering, June 23-28, Oslo, Norway, 2002.
8. Propellant Slosh Loads, NASA SP-8009, August 1968.
9. Slosh Suppression, NASA SP-8031, May 1969.
10. **Warnitchai, P. and Pinkaew, T.,** "Modelling of Liquid Sloshing in Rectangular Tanks with Flow-Dampening Devices," Engineering Structures, Vol. 20, No. 7, 593-600, 1998.
11. **Cho, J.R. and Lee, H.W.,** "Numerical Study on Liquid Sloshing in Baffled Tank by Nonlinear Finite Element Method," Computer Methods in Applied Mechanics and Engineering, Vol. 193, 2581-2598, 2004.
12. **Cho, J.R., Lee, H.W. and Ha, S.Y.,** "Finite Element Analysis of Resonant Sloshing Response in 2-D Baffled Tank," Journal of Sound and Vibration, in press.
13. **Choun, Y-S., and Yun, C-B.,** "Sloshing Characteristics in Rectangular Tanks with a Submerged Block," Computers and Structures, Vol. 61, No. 3, pp. 401-413, 1996.
14. **Biswal, K.C., Bhattacharyya, S.K. and Sinha, P.K.,** "Dynamic Characteristics of Liquid Filled Rectangular Tank with Baffles," The Institution of Engineers (India), Vol. 84, 145-148, 2003.
15. **Evans, D.V. and McIver, P.,** "Resonant Frequencies in a Container with a Vertical Baffle," Journal of Fluid Mechanics, Vol. 175, 295-307, 1987.
16. **Haroun, M.A. and Housner, G.W.,** "Dynamic Characteristics of Liquid Storage Tanks," Journal of Engineering Mechanics, ASCE, Vol. 108, No. EM5, 783-800, 1982.